Optimization of Friction and Electrical Resistance Performance in Graphite-Copper Electrical Contacts Using Taguchi-based Grey Relational Analysis

Djamel Bekhouche
Associate-Professor
Department of Mechanical Engineering
Constantine 1 - Frères Mentouri University
Constantine
Algeria

Ali Bouchoucha
Full Professor
Department of Mechanical Engineering
Constantine 1 - Frères Mentouri University
Constantine
Algeria

Hamid Zaidi
Full Professor
Institut Pprime UPR3346-IUT, Université de Poitiers, Futuroscope, F-86960, Poitiers
France

This study aims to investigate how the load, the intensity, and the polarity of electric current influence the frictional behavior and electrical resistance between a graphite pin loaded against a rotating copper disc. A pin-on-cylinder tribometer was utilized to achieve this. A gray relational grade obtained from gray relational analysis was employed to assess the performance characteristic in the Taguchi mixed L18 (2^1 x 3^2) method. The Taguchi design method determined the optimal control factors that affect the friction coefficient and electrical resistance. Analysis of variance (ANOVA) was employed to analyze the effects of the control parameters on the friction coefficient and electrical resistance of the contact. The experiment parameters included applied normal load (3, 5.5, and 8.5 N), electrical current (10, 25, and 30 A), and polarity (cathode and anode). The analysis results indicated that the polarity was the primary factor influencing the friction coefficient, while the electrical current was the most effective factor in the electrical resistance of the contact. The optimal control parameters for achieving the lowest friction coefficient values were X1Y3Z1, while for the lowest electrical resistance values were X2Y3Z3. Based on the gray relational analysis results, the optimal parameters for minimizing both the friction coefficient and electrical resistance were X1Y3Z1.

Keywords: *Taguchi design, Electric current, Graphite, Friction coefficient, Electrical resistance, Grey relational analysis.*

1. INTRODUCTION

In the field of tribology, electrical current significantly affects the frictional behavior of sliding contacts in motors, railway pantographs, and connectors, showing both positive and negative impacts. Conversely, various studies [1-3] have underscored the pivotal role of electrical current as a crucial parameter influencing thermal processes, kinetic-chemical phenomena, and geometric alterations. Alternatively, given the signi–ficant impact of electric current on the physical and chemical properties of the interface of the graphite-copper contact, research has garnered considerable attention and continues up until today [2, 4-6]. The interaction between the electrical current and the contact surfaces can lead to phenomena like electrical arcing, material transfer, and wear [1, 7]. These phenomena have a direct impact on the performance and reliability of contacts. Understanding the tribological behavior of contacts is crucial for designing and optimizing contact systems. Poljanec et al. [7] confirmed that the electric current can impact contact behavior positively or negatively, with outcomes highly dependent on the selected materials and other contact parameters. The tribological behavior and contact resistance are considered system properties rather than material pro–perties, indicating that they arise from the interaction between two surfaces in relative motion within a particular environment and under specific conditions [8]. The characteristics of tribofilms formed on sliding surfaces play a crucial role in determining friction, contact resistance [9], and the transfer of current, as the significance of film resistance in current transfer is widely recognized [10,11]. It has been observed that friction and electrical current generate heat at the interface, leading to a reduction in the energy of bonds between the contacting materials. This promotes the growth of an oxide film, thereby facilitating sliding [10, 12,13]. It has been found that the intensive current would cause more severe fluctuations in contact resis–tance, while it could extend the operational longevity of the electrical contact system [14]. The surface texture becomes more intricate. Specifically, the roughness of the contact surface alters [15, 16]. On the other hand, although the electrical current may increase the thickness of the oxide layer and create a lubricating film on the contact surface, it also increases contact resis–tance [17]. Certainly, various research papers and reports delve into the effect of load on the tribological behavior of electrical contacts. Some studies have focused on the influence of normal load on the tribological behavior and contact resistance of electrical contacts [7]. D. Wang et al. [1] they found that as the normal load increase, both the friction coefficient and

Received: August 2024, Accepted: October 2024
Correspondence to: Dr Djamel Bekhouche
Department of Mechanical Engineering, Constantine 1 - Frères Mentouri University, Constantine, Algeria
E-mail: djamel.bekhouche@umc.edu.dz
doi: 10.5937/fme2404628B

contact voltage drop exhibit a decreasing pattern. This is because higher loads can promote better electrical contact and reduce the formation of insulating oxide layers on the contact surfaces [7,18]. Liu et al. [19] confirmed that increasing the normal load has a positive effect on reducing both the friction coefficient and contact resistance. Moreover, they observed that while the contact area doesn't infinitely expand, it does reach a stable value as the loads increase. Similar findings were found by Poljanec et al. [7] and Cui et al. [20]. Also, the contact pressure can affect the material transfer between the contacts, further impacting their tribological behavior [7,8,18].

The influence of polarity on friction behavior in electrical contacts can vary based on the specific materials used, environmental conditions, contact design, and the magnitude and duration of the electrical current [7,13]. Detailed studies and experiments under controlled conditions are often necessary to thoroughly understand and characterize the effects of polarity on the tribological behavior of electrical contacts and to establish reliable guidelines for contact system design. Some studies have shown that the friction coefficient can be influenced by the polarity of the electrical current [7,18]. In certain contact materials, the friction coefficient may increase when the current flows in one direction and decrease when it flows in the opposite direction. This phenomenon is attributed to the formation of oxide layers on the contact surfaces, which can affect the adhesion and friction between the contacts [7,21].

Many researchers have focused on investigating the impact of individual parameters or a set of fixed parameters on the tribological characteristics of sliding electrical contacts. However, this approach may not be suitable for specific scenarios where the combined effects of interacting parameters are significant. In fact, The Taguchi methodology for optimization is widely favored and highly regarded in current research. It enables optimization with fewer investigations, eliminates biases, promotes cost-effectiveness, improves quality, and leads to robust designs.

In addition to this, the gray relational analysis method (GRA) has been used to identify the optimal controllable variables for a multi-objective function. This approach simplifies the intricate process of multi-objective optimization into a single response, referred to as a relational grade. In this study, we aimed to identify the optimal parameters (load, electrical current, and polarity) to simultaneously optimize both friction coefficient (COF) and electrical resistance (Rc) using the Grey Taguchi method. The optimized parameters were subsequently validated through a confirmation experiment.

2. EXPERIMENTATION AND MATERIAL

2.1 Testing materials

The cylinders are made of 99.98% pure copper (refers to a high purity level of copper), which is an excellent conductor of heat and electricity. Its FCC structure makes it malleable and ductile, easily deformable at cold temperatures, with recrystallization starting at around 220°C. The pin specimens are made from artificial graphite, also known as electrographite. In fact, graphite is a unique form of carbon known for its distinct properties and various applications. It's a crystalline form of carbon where each carbon atom is bonded to three other carbon atoms, forming flat hexagonal sheets. These sheets stack on top of each other with weak bonds between them, giving graphite its unique characteristics. it's extensively used in industries to produce solid lubricants because of its layered structure, which allows easy sliding between the sheets [22]. The primary mechanical and physical characteristics of the chosen materials are outlined in Table 1.

Table 1. Mechanical and physical characteristics of the used materials

Material	E	ρ	γ	K
Copper	126	8.9	1.682	385.8
Electrographite	10.25	2.26	8-13	124-168

2.2 Experimental apparatus

The friction tests were conducted on a pin-on-cylinder tribometer using the rotation sliding mode. Figure 1 illustrates the schematic testing setup and the electrical circuit applied for conducting the sliding electrical contact experiments.

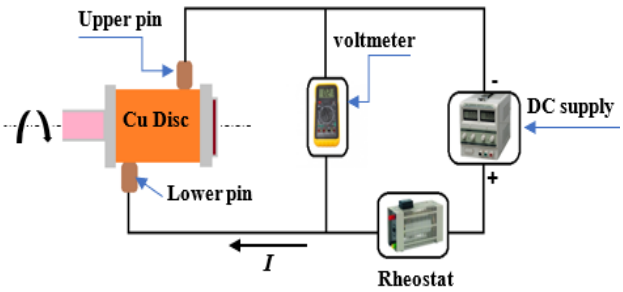

Figure 1. Schematic illustration of experimental setup

The pin specimen was fixed in an insulated upper holder within the tribometer's arm. In contrast, another pin, connected to a DC power source, was placed in the lower holder to enable electrical conduction. A consistent normal load between the specimens was achieved using dead weights.

The computer automatically recorded real-time friction coefficient (COF) curves over sliding time. The cylinder sample, crafted from copper and measuring 45 mm in diameter, is mounted onto a disc holder within the lathe's mandrel. A pin made from graphite, with a cylindrical shape covering 8 mm in diameter and 20 mm in length, supports the cylinder under a normal load P. Before each test, the copper surface underwent polishing using abrasive paper ranging from 800 to 2000 grit, followed by cleaning with alcohol. Similarly, the graphite pin specimen was polished using 1200-grade abrasive paper to ensure optimal surface contact. The tests were conducted in ambient air conditions, with a dry environment and an approximate temperature of 22°C.

2.3 Taguchi optimization method

Optimizing process parameters and understanding their individual contributions can be effectively accomplis–

hed by implementing a mixed-level orthogonal array (OA) such as the Taguchi L18 (2^1 x 3^2) mixed design. This approach enables a systematic evaluation of single parameters and their impact on the system's overall performance under study. The structured arrangement of experiments within the orthogonal array facilitates the identification of key factors influencing the desired outcomes, leading to informed decision-making in process optimization. The Taguchi method is utilized for optimizing process parameters, and in this study, three parameters are considered, with two parameters having three levels and one parameter with two levels (2^1 x 3^2), as shown in Table 2. Eighteen trials were conducted based on the Taguchi L18 (2^1 x 3^2) OA, as detailed in Table 3.

Table 2. Experimental parameters, along with their corresponding levels

Parameters	Symbol	Level		
		1	2	3
Polarity	X	A	C	-
Electrical current, I (A)	Y	10	20	30
Load, P (N)	Z	3	5.5	8.5

A: Anode polarity and **C:** Cathode polarity

The Taguchi method was selected due to its ease of analysis, significant cost reduction in experiments, and validity across a broad range of control factors and their settings [23]. Signal-to-noise ratios (SNRs) are employed to identify the optimal parameters, with three quality characteristic categories for SNRs: smaller is better, nominal is best, and larger is better. Therefore, to achieve optimal friction coefficient (COF) and electrical resistance (Rc) parameters in this study, the smaller-is-better function is utilized. SNRs for COF and Rc were computed using equation (1) for all 18 trials. The signal-to-noise (S/N) ratio for each factor level combination is calculated using the smaller-is-better S/N ratio formula with base 10 log.

$$S/N = -10\log\left(\frac{1}{m}\sum_{i=1}^{m} y_i^2\right) \tag{1}$$

In this equation, y represents the responses corresponding to the specific factor level combination, while m denotes the total number of responses in that combination.

2.4 Gray relational analysis

Grey relational analysis (GRA) is a methodology employed for optimizing multiple input parameters to achieve optimal quality derived from grey system theory [24-25]. Initially proposed by J. Deng [25], GRA has found extensive applications across diverse fields. It is a novel approach for analyzing systems that may not be effectively analyzed using traditional statistical methods, particularly in situations involving uncertainty or partial information [26].

The normalization process is designed based on the experiment's objective, whether the response variables are aimed to be minimized or maximized. In this case, both the friction coefficient and electrical resistance are targeted for minimization. To normalize the two responses, the following smaller is better formula can be used (2):

$$x_i(k) = \frac{\max x_i^0(k) - x_i^0(k)}{\max x_i^0(k) - \min x_i^0(k)} \tag{2}$$

This equation $x_i^0(k)$ represents the value post-grey relational generation, and x^0 denotes the desired value.

Grey relational coefficients are computed to depict the correlation between the ideal and the actual experimental outcomes. The grey relational coefficient is determined from the normalized values using the equation (3):

$$\gamma_i(k) = \frac{\min\limits_j \min\limits_k \left|x_0(k) - x_j(k)\right| + \zeta \max\limits_j \max\limits_k \left|x_0(k) - x_j(k)\right|}{\left|x_0(k) - x_j(k)\right| + \zeta \max\limits_j \max\limits_k \left|x_0(k) - x_j(k)\right|} \tag{3}$$

Here ζ is the adjustment coefficient used to modify the relational coefficient difference, typically where r $\in$ {0, 1} [25]. In fact, the recommended value for the distinguishing coefficient is set at 0.5, chosen for its moderate distinguishing effects and reliable stability in outcomes. Hence ζ, 0.5 is selected for further analysis in this particular case.

After calculating the grey relational coefficient, we compute the Grey relational grade for each performance characteristic. This grade is determined using equation (4):

$$\phi_i = \frac{1}{n}\sum_{k=1}^{n} \gamma_i(k) \tag{4}$$

Here, ϕ_i denote the grey relational grade for each experiment, with n representing the number of performance characteristics.

3. RESULTS AND DISCUSSION

3.1 Experimental analysis

Table 3 presents the experimental results regarding the friction coefficient and electrical contact resistance, as acquired through the mixed Taguchi L18 experimental design. The effect of the applied normal load, the electrical current, and its polarity on the friction coefficient and the electrical resistance of contact are shown in Figure 2. As shown in Figure 2(a), the friction coefficient of the contact exhibits a slight increase with the rise in normal load when subjected to anodic polarity. Conversely, when the pin is a cathode, the friction coefficient shows a slight decrease as the normal load increases. Furthermore, we look at the influence of electrical current. The experimental results show that the friction coefficient decreases with the increase of the electrical current, regardless of the polarity. On the other hand, the friction coefficient under cathodic polarity is more important than under anodic polarity.

Figure 2(b) shows that the effect of applied normal load on the electrical resistance of contact is very small. As we can see, the effect of electrical current and its polarity is very clear. In fact, the electrical resistance of contact decreases with an increase in electrical current, regardless of polarity. Furthermore, the difference between the values of the electrical contact resistance

under the effect of anodic polarity is more pronounced than that of the cathodic polarity.

Table 3. The experimental results via the mixed Taguchi L18 experimental design

Exp. N°	Control parameters			Response parameters	
	X Polarity	Y I (A)	Z P (N)	COF	Rc (mΩ)
1	A	10	3.0	0.216	128.73
2	A	10	5.5	0.227	127.62
3	A	10	8.5	0.223	127.23
4	A	20	3.0	0.180	63.82
5	A	20	5.5	0.220	61.07
6	A	20	8.5	0.214	58.89
7	A	30	3.0	0.164	40.25
8	A	30	5.5	0.200	37.23
9	A	30	8.5	0.196	33.38
10	C	10	3.0	0.305	58.75
11	C	10	5.5	0.292	49.67
12	C	10	8.5	0.276	41.67
13	C	20	3.0	0.296	36.56
14	C	20	5.5	0.277	32.15
15	C	20	8.5	0.268	28.30
16	C	30	3.0	0.260	27.29
17	C	30	5.5	0.261	23.18
18	C	30	8.5	0.250	20.42

In the presence of electrical current, an elevated normal load leads to a decrease in contact resistance, primarily because it enlarges the real contact area, thereby facilitating a reduction in contact resistance throughout the contact surface, which contributes to improved tribological performance in electrical sliding contacts, with specific consideration given to the properties of each material involved [27, 7]. The experimental findings reveal a significant impact of electrical current and its polarity on the frictional behavior of the graphite-copper couple, directly influencing its lifetime. In fact, this parameter exerts a notable influence, particularly on the oxidation process occurring on the contacting surfaces.

In Figures 3 and 4, SEM and EDX analyses were conducted on the worn surfaces of the pin on graphite. These figures reveal the presence of an oxygen element peak, confirming an oxidizing reaction occurred, along with various other elements. This phenomenon is attri–buted to mutual transfer between the antagonist sur–faces, as identified by EDX analysis. Alongside the heat generated from friction and the Joule effect, the elec–trical current intensity creates an electric field at the interface. This field triggers the anode material's oxida–tion, while the oxide film's growth diminishes the elec–tric field intensity [28]. Consequently, the oxide film expands until it breaks mechanically and/or elect–rically (arcing). Under certain operational conditions, this film adapts effectively to copper irregularities, safeguarding it from damage. Notably, when the pin acts as the cathode, the friction coefficient variations are more pronounced than an anode pin [27].

The flow of electrical current through the contact results in the creation of an electric field, the strength of which correlates directly with the current intensity and the electrical contact resistance [18, 29]. In contrast, the contact resistance decreases as the normal load incr–eases. As the load decreases, the electric field becomes stronger, leading to a heightened impact of the current on the friction characteristics, particularly in the case of graphite, when the load decreases.

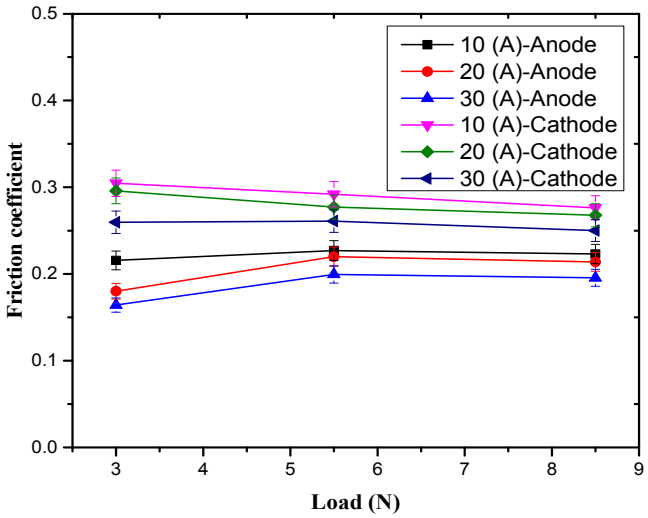

a)

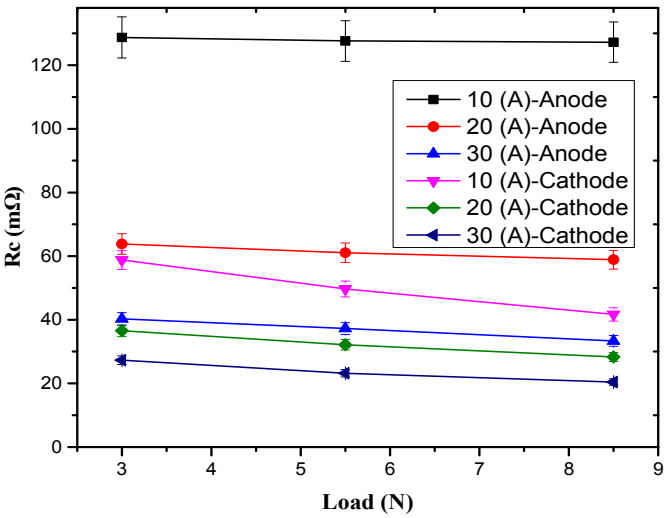

b)

Figure 2. Experimental effect of the control parameters on a) COF and b) Rc, v= 4 m/s

The diffusion process regulates the rate of oxidation through the surface layers. This diffusion within the oxide layer is influenced by the density of defects and the intensity of the contact electric field. As the oxide film grows, it leads to a reduction in the contact electric field and an increase in the maximum shear stresses experienced by the contact [7, 30]. The critical thickness required for film rupture may result from either shearing forces or electrical breakdown.

Conversely, as the contact electrical resistance increases, the friction coefficient decreases simulta–neously. This phenomenon suggests the formation of an impurity deposit on the surfaces, likely a combination of transferred metal oxides and wear particles from the surfaces (as confirmed in Figure 3(a)), which act as a lubricating agent. Film rupture occurs cyclically, initiating from a critical thickness characterized by a variation in the electrical contact resistance.

In contrast, during periods of increased friction coefficient, oxide film rupture is probable (leading to an increase in friction coefficient), attributed to mechanical and/or electrical influences [31].

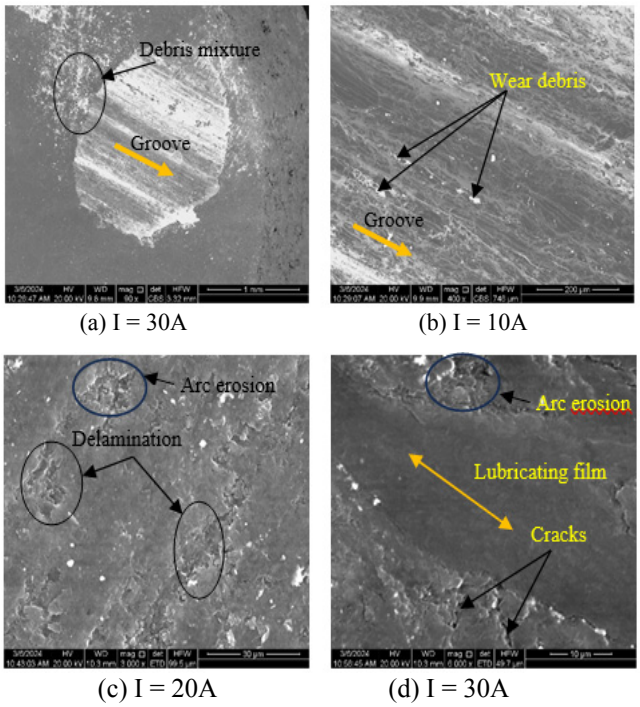

(a) I = 30A (b) I = 10A

(c) I = 20A (d) I = 30A

Figure 3. SEM micrographs of worn surfaces of graphite pin v = 4 m/s, P = 8.5

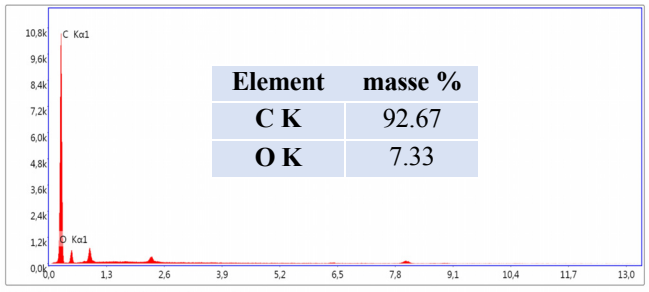

(a) I = 10A

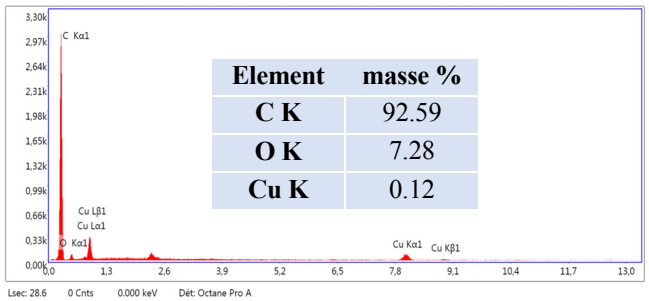

(b) I = 20A

Figure 4. EDX spectra of graphite worn surface v = 4 m/s, P = 8.5 N

3.2 Statistical analysis

Tables 4 and 5 present the response outcomes of the S/N ratio concerning both the friction coefficient and the electrical resistance of contact obtained by using the Taguchi method. It outlines the S/N ratio associated with each control parameter across different levels. The numerical labels 1, 2, and 3 represent the average results of the experiments for each factor at their corresponding level. Furthermore, the term 'Delta' indicates the variation between each control factor's highest and lowest S/N ratios across the three levels, offering insight into the primary and secondary levels of influence for each factor within the experimental findings.

Table 4. Response table for S/N ratio for COF

	Friction coefficient (COF)		
Level	Polarity	I (A)	P (N)
1	13.84	11.90	12.75
2	11.20	12.43	12.25
3	-	13.21	12.54
Delta	2.64	1.31	0.50
Rank	1	2	3

Table 5. Response table for S/N ratio for Rc

	Electrical resistance (Rc)		
Level	Polarity	I (A)	P (N)
1	-36.40	-38.02	-34.29
2	-30.48	-32.94	-33.44
3	-	-29.37	-32.60
Delta	5.11	8.65	1.69
Rank	2	1	3

According to the findings in Table 4, the S/N ratio at the anodic and cathodic polarity levels for the friction coefficient is 2.64, the highest among the three S/N ratio values. Conversely, the S/N ratio at applied load levels yields the smallest value of 0.50. In fact, a notable change in the friction coefficient is observed with the increasing interval from 10 to 30 (A) in electrical current, regardless of the polarity. On the other hand, the electrical resistance contact exhibits the highest S/N ratio of 8.65 between electrical current levels of 10, 20, and 30 (A) and the lowest ratio of 1.69 between load levels of 3, 3.5, and 8.5 (N), highlighting electrical current as the primary influencing factor and load as the least influential (Table 5). Hence, the sequence of inf–luence factors on the friction coefficient can be arranged as follows: Polarity > Electrical current > Load, while on electrical resistance contact: Electrical current > Po–larity > Load.

Following the analysis of the S/N ratio, it becomes evident that electrical current and its polarity exert the most significant influence on both the friction coef–ficient and electrical resistance contact. The level values of control factors for these properties, as presented in Tables 4 and 5, are graphically depicted in Figures 5 and 6. These graphical representations facilitate the easy determination of optimal parameters for minimizing or obtaining better friction coefficient and electrical resistance contact.

In fact, at the optimum condition, S/N ratios should consistently be maximized. Consequently, the levels and associated S/N ratios for achieving the best friction coefficient value are specified as follows: electrical current (30 A, S/N = 13.21), load (3 N, S/N = 12.75), and polarity (anode, S/N = 13.84). Similarly, for elec–trical resistance contact, the optimal parameter combi–nation comprises electrical current (30 A, S/N = -29.37), load (8.5 N, S/N = -32.60), and polarity (cathode, S/N = -30.48).

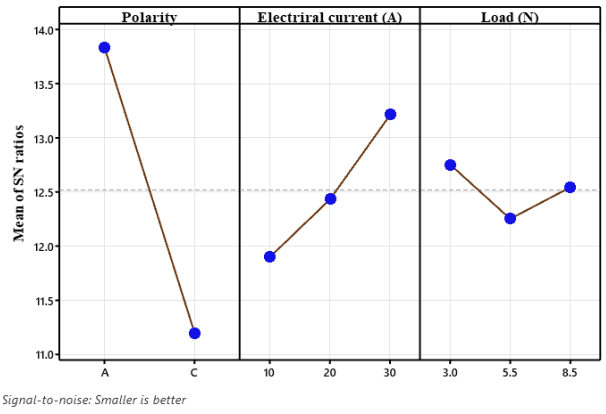

Figure 5. Control parameter effects on average S/N ratio for COF

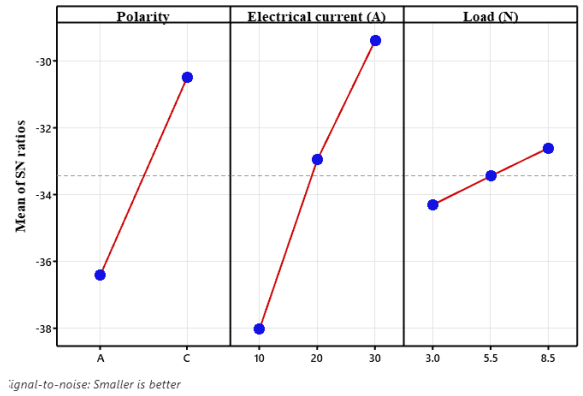

Figure 6. Control parameter effects on average S/N ratio for Rc

ANOVA, or Analysis of Variance, serves as a statis–tical tool employed to assess the distinct interactions among all the control factors within a given experi–mental design. In this research, ANOVA was applied to examine and analyze the impacts of electrical current, applied normal load, and polarity on both the friction coefficient and the electrical resistance of contact. In fact, the analysis was performed with a significance level of 5% and a confidence level of 95%. Assessing the significance of control factors in ANOVA entails comparing the F values associated with each control factor [32]. The ANOVA results for the friction coef–ficient and the electrical resistance of contact are shown in Tables 6 and 7, respectively.

The computed F values for the influential factors are presented in these tables. As depicted, the degree of freedom for the polarity factor was 1, while for the other two influential factors, it was 2. Additionally, the degree of freedom for the error was 12 for both the friction coefficient and the electrical resistance of contact. The last column of the table shows the percentage value of each parameter contribution, which indicates the degree of influence on the process performance. In Table 6, it can be seen that the polarity has a greater influence of 78.45%, the electrical current has an influence of 12.51%, and the load has an influence of 1.10%. Thus, the most important factor affecting the friction coefficient of the contact was the polarity (contribution of 78.45%). In Table 7, according to the ANOVA results, it's obvious that the electrical current, polarity, and load have percentage contributions of 50.30%, 33.03%, and 0.79%, respectively. This showed that the electrical current and polarity were the most effective factors in electrical resistance.

The normal probability graph, also known as a nor–mal probability plot or normal Q-Q plot, is a graphical method used to assess whether a dataset follows a normal distribution [33]. When points cluster closely around the line, it indicates minimal deviation [34]. Figure 7 displays residual graphs for the friction coef–ficient and electrical resistance contact. The nearly li–near response observed in the normal probability graph suggests that errors follow a normal distribution. This suggests that the proposed model closely aligns with the experimental values.

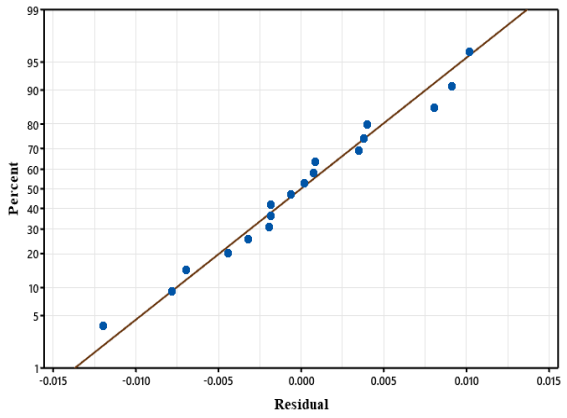

(a)

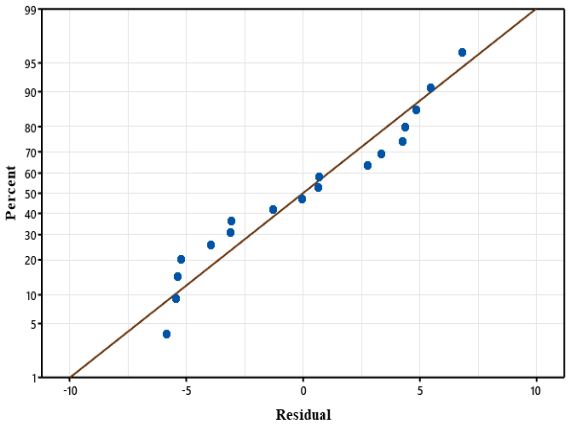

(b)

Figure 7. Normal probability graph for the S/N ratios of a) COF and b) Rc

Table. 6 Analysis of Variance for friction coefficient

Source	DF	Seq SS	Adj SS	Adj MS	F-Value	P-Value	Contribution
Polarity	1	0.023127	0.023127	0.023127	118.74	0.0000001	78.45%
Electrical current (A)	2	0.003689	0.003689	0.001845	9.47	0.0034027	12.51%
Load (N)	2	0.000325	0.000325	0.000162	0.83	0.4580018	1.10%
Error	12	0.002337	0.002337	0.000195	-	-	7.93%
Total	17	0.029478	-	-	-	-	100.00%

Table. 7 Analysis of Variance for electrical resistance

Source	DF	Seq SS	Adj SS	Adj MS	F-Value	P-Value	Contribution
Polarity	1	7208.6	7208.6	7208.61	24.96	0.00031	33.03%
Electrical current (A)	2	10979.0	10979.0	5489.51	19.01	0.00019	50.30%
Load (N)	2	173.0	173.0	86.51	0.30	0.74657	0.79%
Error	12	3466.1	3466.1	288.84	-	-	15.88%
Total	17	21826.7	-	-	-	-	100.00%

Table. 8 Predicted equations of COF and Rc

	Friction coefficient
Anode (linear)	COF = 0.2387 - 0.001743 Y + 0.00010 Z
Cathode (linear)	COF = 0.3104 - 0.001743 Y + 0.00010 Z
	R-sq 90.82%
Anode (quadratic)	COF = 0.1924 - 0.00159 Y + 0.02249 Z - 0.000034 Y^2 - 0.001202 Z^2 + 0.000076 XY- 0.00819 XZ + 0.000190 YZ
Cathode (quadratic)	COF = 0.3090 - 0.00159 Y + 0.02249 Z - 0.000034 Y^2 - 0.001202 Z^2 + 0.000076 XY - 0.00819 XZ + 0.000190 YZ
	R-sq 98.00%
	Electrical resistance
Anode (linear)	Rc (mΩ) = 141.8 - 2.933 Y - 1.37 Z
Cathode (linear)	Rc (mΩ) = 101.8 - 2.933 Y- 1.37 Z
	R-sq 81.10%
Anode (quadratic)	Rc (mΩ) = 218.4 - 13.02 Y - 1.08 Z + 0.1282 Y^2 + 0.084 Z^2 + 3.225 XY - 1.14 XZ + 0.0217 YZ
Cathode (quadratic)	Rc (mΩ) = 120.3 - 13.02 Y - 1.08 Z + 0.1282 Y^2 + 0.084 Z^2 + 3.225 XY - 1.14 XZ + 0.0217 YZ
	R-sq 98.56%%

A linear and quadratic regression was utilized to model the correlation between the control factors and the performance measures. In fact, these analyses offer a robust method for examining variables, especially when a relationship exists between dependent and inde–pendent variables [35].

This context's dependent variables were electrical current, load, and polarity. In contrast, the performance measurements, serving as the independent variables, were defined as friction coefficient and electrical resis–tance contact. The resulting regression equations are outlined in Table 8.

The predicted linear and quadratic equations for the output responses are shown in Table 8. The R^2 values obtained from the linear regression model equations were 90.82% for the friction coefficient and 81.10% for electrical resistance contact.

Figure 8 displays a comparison between predicted values from the quadratic regression model and experi–mental results, indicating a strong correlation. The quadratic regression model yielded R^2 values of 98.00% for the friction coefficient and 98.56% for electrical resistance contact. Generally, closer proximity to 1 in the R^2 value signifies a better model fit [36]. Notably, the predicted values derived from the quadratic regression model exhibited higher precision compared to those from the linear regression model, demonstrating the effecti–veness of the quadratic regression model in predicting friction coefficient and electrical resistance contact.

Figure 9 illustrates the 3D response surface estimation for the friction coefficient (COF) in relation to control factors out of electrical current, polarity, and applied load. In Figure 9(a), it's apparent that the friction coefficient tends to decrease as a convex shape, with an increase in electrical current. In fact, the influence of electrical current on the friction coefficient is considerably significant compared to the applied normal load, wherein the highest friction coefficient is observed at the lowest electrical current (10 A) under the 5.5 N applied load value. Figure 9(b) presents a similar relationship, this time focusing on polarity and electrical current. Here, the friction coefficient reaches its minimum value at the highest electrical current (30 A) under anodic polarity and vice versa.

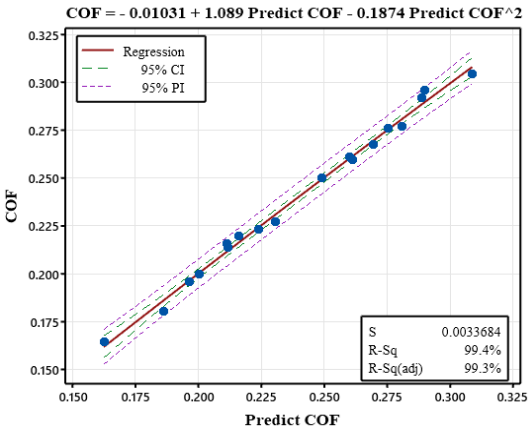

(a)

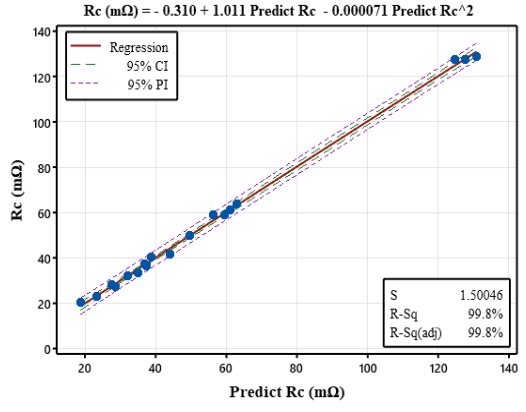

(b)

Figure 8. The compared experimental results with the quadratic regression model for a) COF and b) Rc

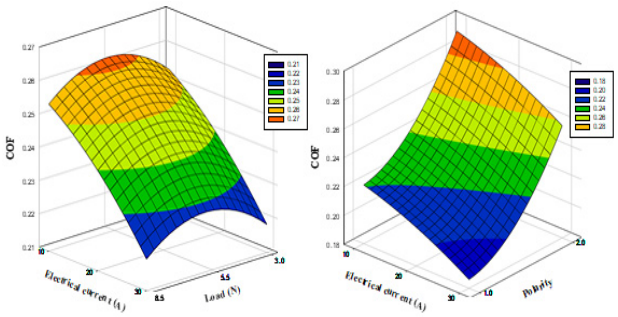

(a) (b)

Figure 9. 3D plot of the influence of interactions of control factors on COF

The contour plots presented in Figure 10 illustrate the 3D response surfaces for the electrical resistance contact in relation to pairs (control factors) of electrical current, applied load, and polarity. Specifically, in Figure 10(a), it is observed that electrical resistance contact follows a concave shape, decreasing as both electrical current and applied load increase. In fact, the combination of the highest electrical current and applied load yields the minimum resistance and vice versa. Additionally, Figure 10(b) demonstrates that the electrical resistance contact attains its maximum value at the lowest electrical current (10 N) under anodic polarity, while its lowest value is observed at the highest electrical current (30 A) under cathodic polarity.

To successfully conduct this study, a confirmation testing of the process parameters at both optimal and random levels was conducted using the Taguchi techni–que and predictive regression equations. Table 9 pre–sents the comparison between test results and predicted values obtained from both the Taguchi method and reg–ression equations. The experimental outcomes closely align with the predicted values. In fact, it has been reported that, for statistical analysis to be considered reliable, error values should not exceed 20% [37], a finding confirmed in Table 9. Based on the results obtained, it is evident that the quadratic model is highly accurate.

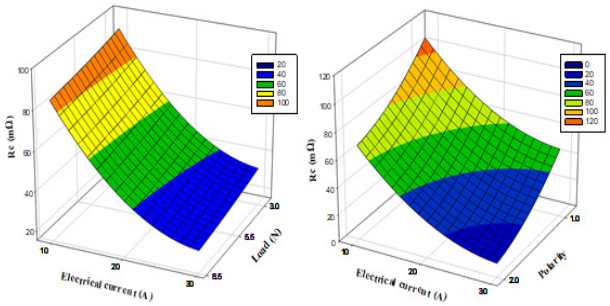

(a) (b)

Figure 10. The 3D plot of the influence of interactions of control factors on Rc

3.3 GRA method for COF and Rc

The grey relational grade quantifies the similarity between comparability and reference sequences. Attaining the highest grey relational grade with the reference sequence indicates the comparability sequence's close resemblance, rendering it the optimal choice for experimentation [24, 38]. The friction coefficient and the electrical resistance results shown in Table 3 undergo normalization using equation (2). Subsequently, the Grey relational coefficient is computed for each response utilizing equation (3). The resulting gray relational grade and corresponding experiment rankings are detailed in Table 10. Notably, the maximum grey relational grade corresponds to the highest gray relational grades, indicated by number 1 in the ranking column [39]. In fact, experiment number 7, indicated in Table 10, signifies the closest combination of optimal controllable parameters of this study (X1Y3Z1): anodic polarity, an electrical current of 30 (A), and an applied load of 3 (N).

Table. 9 The comparisons of predicted values and confirmation test results.

Exp. N°	Parameters			For Taguchi method			For regression equations		
	Polarity	I (A)	P (N)	Exp.	Pred.	Error (%)	Exp.	Pred.	Error (%)
COF									
1 (Optimum)	A	30	3	0.164	0.164	0.00	0.164	0.165	-0.60
2 (Random)	C	10	5.5	0.292	0.291	0.34	0.292	0.298	-2.05
3 (Random)	A	20	8.5	0.214	0.212	0.93	0.214	0.215	-0.46
Rc									
1 (Optimum)	C	30	8.5	20.42	18.728	8.28	20.42	21.62	-5.87
2 (Random)	A	10	3	128.73	131.01	-1.77	128.73	128.01	0.56
3 (Random)	A	20	8.5	58.89	59.56	-1.13	58.89	64.66	-9.79

Table 10 Grey relational analysis for COF and Rc.

Exp. N°	Normalized experimental		Deviation sequences		GRC		GRG	GRG Rank
	COF	Rc	COF	Rc				
1	0.6312	0.0000	0.3688	1.0000	0.5755	0.3333	0.4544	16
2	0.5532	0.0102	0.4468	0.9898	0.5281	0.3356	0.4319	18
3	0.5816	0.0138	0.4184	0.9862	0.5444	0.3364	0.4404	17
4	0.8865	0.5993	0.1135	0.4007	0.8150	0.5551	0.6851	6
5	0.6028	0.6247	0.3972	0.3753	0.5573	0.5712	0.5643	11
6	0.6454	0.6448	0.3546	0.3552	0.5851	0.5847	0.5849	10
7	1.0000	0.8169	0.0000	0.1831	1.0000	0.7320	0.8660	1
8	0.7447	0.8448	0.2553	0.1552	0.6620	0.7631	0.7125	4
9	0.7730	0.8803	0.2270	0.1197	0.6878	0.8069	0.7474	2

10	0.0000	0.6461	1.0000	0.3539	0.3333	0.5856	0.4594	15
11	0.0922	0.7299	0.9078	0.2701	0.3552	0.6493	0.5022	14
12	0.2057	0.8038	0.7943	0.1962	0.3863	0.7182	0.5522	13
13	0.0638	0.8510	0.9362	0.1490	0.3481	0.7704	0.5593	12
14	0.1986	0.8917	0.8014	0.1083	0.3842	0.8220	0.6031	9
15	0.2624	0.9272	0.7376	0.0728	0.4040	0.8730	0.6385	8
16	0.3191	0.9366	0.6809	0.0634	0.4234	0.8874	0.6554	7
17	0.3121	0.9745	0.6879	0.0255	0.4209	0.9515	0.6862	5
18	0.3901	1.0000	0.6099	0.0000	0.4505	1.0000	0.7252	3

Table.11 Optimum conditions for COF and Rc

		For Taguchi method				For GRA	
		COF		Rc			
Parameters	Symbol	Best level	Value	Best level	Value	Best level	Value
Polarity	X	1	A	2	C	1	A
I (A)	Y	3	30	3	30	3	30
P (N)	Z	1	3	3	8.5	1	3

Based on the results obtained, Table 11 displays the optimal levels of control parameters determined through the analyses.

4. CONCLUSION

This study utilized Taguchi's orthogonal array combined with grey relational analysis to optimize the graphite-copper electrical couple's friction coefficient and electrical resistance contact. From the experimental findings, the following conclusions were derived:

The findings of this study underscore the significant influence of electric current and its polarity on the frictional characteristics of the graphite-copper contact. Additionally, the observation of an O peak in the EDS spectra of the worn surfaces indicates the occurrence of an oxidizing reaction, effectively acting as a lubricant, similar to the function of a solid lubricant.

The study used signal-to-noise (S/N) ratios to iden–tify the optimal control factor levels to minimize both friction coefficient and electrical contact resistance.

The study established that the optimal parameters for achieving the best results in terms of friction coefficient and electrical contact resistance were determined at X1Y3Z1 (anodic polarity, 30 A and 3 N) and X2Y3Z3 (cathodic polarity, 30 A and 8.5 N), respectively.

The statistical analyses indicated that the polarity and electrical current exhibited the highest levels of sig–nificance concerning the friction coefficient and elec–trical resistance of the contact, contributing to 78.45% and 50.30% of the variance, respectively.

The application of Grey Relational Analysis within the Taguchi method is a highly effective tool for optimizing multi-response problems, particularly in predicting the graphite-copper couple's friction coefficient and electrical resistance. The optimal parameters for minimizing both the friction coefficient and electrical resistance were X1Y3Z1.

The comparison between the experimental and predicted values of the friction coefficient and electrical resistance demonstrates a high level of agreement, indicating the accuracy of the developed model. Consequently, the model is deemed reasonably accurate and can be confidently recommended for predicting the tribological behavior of electrical contacts.

REFERENCES

[1] Wang, D., Chen, X., Li, F., Chen W., Li H., Yao, C.: Influence of normal load, electric current and sliding speed on tribological performance of electrical contact interface, Microelectronics Reliability, Vol, 142, pp. 114929, 2023. https://doi. org/10.1016/j.microrel.2023.114929

[2] Wang, C., Xiao, JK., Xiao, SX., Xu, GM., Chen, J., Zhang, C.: Effect of Electrical Current on the Tribological Property of Cu-Graphite Brush, Tribology Letters, Vol. 72, pp. 29, 2024. https:// doi.org/10.1007 /s11 249-023-01825-1

[3] Kloch, K.T., Kozak, P., Mlyniec, A.: A review and perspectives on predicting the performance and durability of electrical contacts in automotive applications, Eng. Fail. Anal. Vol. 121, pp. 105143, 2021.

[4] Rajkumar, K., Aravindan, S.: Tribological behavior of microwave processed copper-nanographite composites, Tribol. Int, Vol. 57, pp. 282–96, 203. https://doi.org/10.1016/j.triboint.2012 .06.023

[5] Keshavamurthy, R., Tambrallimath, V., et al.: Friction and Wear Behaviour of Copper Reinforced Acrylonitrile Butadiene Styrene based Polymer Composite Developed by Fused Deposition Modelling Process, FME Transactions, Vol. 48 No. 3, pp. 543-550, 2020.

[6] Sarmadi, H., Kokabi, A.H., Seyed Reihani, S.M.: Friction and wear performance of copper-graphite surface composites fabricated by friction stir processing (FSP), Wear, Vol. 304, pp. 1-12, 2013. https:// doi.org /10.1016 /j. wear.2013.04.023

[7] Poljanec, D., Kalin, M., Kumar, L.: Influence of contact parameters on the tribological behaviour of various graphite/graphite sliding electrical contacts, Wear, Vol. 406–407, pp. 75-83, 2018.

[8] Grandin, M., Wiklund, U.: Influence of mechanical and electrical load on a copper/copper-graphite sliding electrical contact, Tribology International, Vol. 121, pp. 1-9, 2018.

[9] Jacobson, S., Hogmark, S.: Surface modifications in tribological contacts, Wear,Vol. 266, pp. 370-8, 2009.

[10] Holm, R.: *Electric contacts; theory and applications*, fourth ed. Berlin, Springer, 1976.

[11] Slade, PG.: *Electrical contacts, Principles and applications*, CRC Press, 2017.

[12] Bekhouche, D., Bouchoucha, A., Zaidi, H.: Tribological Behavior of a Contact Pin on Cylinder CuSn7 Bronze Rubbing Against 20MnCr5 Steel in Dry Sliding with Electrical Current, J. Mech. Eng, Vol. 16, No. 2, pp. 109–128, 2019.

[13] Paulmier, D., Zaidi, H., Salliot, H., Hounkponou, E.: Effects of electrical current and its polarity on the surfaces of copper and carbon in contact, Surface Science, Vol. 251–252, pp. 769-772, 1991.

[14] Ren, W., Zhang, X., Meng, X.: Fretting behavior of gold-plated contact materials used in high-frequency vibration and different temperature environment, IEEE Trans. Compon. Packag. Manuf. Technol, Vol. 7, No. 4, pp. 572-581, 2017.

[15] Yi, F., Zhang, M., Xu, Y.: Effect of the electric current on the friction and wear properties of the CNT-Ag–G composites, Carbon, Vol. 43, No. 13, pp. 2685-692, 2005.

[16] Zuo, X., Xie, W.X., Zhou, Y.K.: Influence of electric current on the wear topography of electrical contact surfaces, J. Tribol, Vol. 144, No. 7, pp. 071702, 2022.

[17] Hu, Z.L., Chen, Z.H., Xia, J.T.: Study on surface film in the wear of electrographite brushes against copper commutators for variable current and humidity, Wear, Vol. 264, pp. 11–17, 2008.

[18] Xiao, J., Wang, C., Xiao, S., Chen, J., Zhang, C.: Sliding electrical contact properties of highly oriented copper fiber brush, Wear, Vol. 512–513, pp. 204541: 2023.

[19] Liu, X.L., Cai, Z.B., Liu, S.B., Wu, S.B., Zhu M.H.: Influence of wear test parameters on the electrical contact performance of brass alloy/copper contactors under fretting wear, J. Mater. Eng. Perform, Vol. 28, No. 2, pp. 817–827, 2019.

[20] Cui, G., Bi, Q., Yang, J., Liu, W.: Effect of normal loads on tribological properties of bronze-graphite composite under seawater condition, Tribology Transaction, Vol. 57, pp. 308-316, 2014.

[21] Persson, B.N.J.: On the Electric Contact Resistance, Tribology Letters, Vol. 70, pp. 88, 2022. https://doi.org/ 10.1007/s11249-022-01630-2

[22] Bouchoucha, A. : *Etude de comportement en frottement et usure des contacts électriques glissants cuivre-acier et cuivre-graphite*, PhD Thesis, Université Frères Mentouri Constantine, Algeria, 1997.

[23] Freddi, A., Salmon, M.: Introduction to the Taguchi Method. In: Design Principles and Methodologies, *Springer Tracts in Mechanical Engineering*, Springer, Cham, 2019. https://doi.org/10 .1007/978 -3-319-95342-7_7

[24] Sai Ram J, Shiek J, Hameed Syed, S.: Multi-response Optimization of PMEDM on Inconel 718 Using Hybrid T-GRA, TOPSIS, and ANN Model, FME Transactions, Vol. 51, pp. 564-574, 2023.

[25] Deng, J.: Control problems of grey systems, Systems and Control Letters, Vol. 1, pp. 288–294, 1982.

[26] Liu, S., Yang, Y., Forrest, J.YL.: *Grey Relational Analysis Models. In: Grey Systems Analysis*, Series on Grey System. Springer, Singapore, 2022.

[27] Grandin, M., Wiklund, U.: Wear and electrical performance of a slip-ring system with silver-graphite in continuous sliding against PVD coated wires, Wear, Vol. 348–349, pp. 138–147, 2016.

[28] Poljaneca, D., Kalinb, M.: Effect of polarity and various contact pairing combinations of electrographite, polymer-bonded graphite and copper on the performance of sliding electrical contacts, Wear, Vol. 426–427, pp. 1163-1175, 2019.

[29] Csapo, E., Zaidi, H., Paulmier, D., Kadiri, E.K., Bouchoucha, A., Robert, F.: Influence of the electrical current on the graphite surface in an electrical sliding contact, Surface and Coatings Technology, Vol. 76-77, pp. 421-424, 1995.

[30] Mouadji, Y. : *Effet du courant électrique sur le mécanisme de croissance de la couche d'oxyde à l'interface des contacts électrodynamiques cuivre-graphite et graphite-graphite*, PhD Thesis, Université Frères Mentouri Constantine1, Algeria, 2013.

[31] Bouchoucha, A., Zaidi, H., Kadiri, E.K., Paulmier, D.: Influence of electric fields on the tribological behaviour of electrodynamical copper/steel contacts, Wear, Vol. 203-204, pp. 434-441, 1997.

[32] Řehoř, J.: ANOVA analysis for estimating the accuracy and surface roughness of precisely drilled holes of steel 42CrMo4 QT, Int J. Adv. Manuf. Technol, Vol. 126, pp. 675–695, 2023.

[33] Montgomery, D.C, Peck, E.A, Vining, G.G.: *Introduction to Linear Regression Analysis, Wiley series in probability and statistics*, 6th edition, 2021.

[34] Nas, E., Özbek, N.A.: Optimization of the machining parameters in turning of hardened hot work tool steel using cryogenically treated tools, Surface Review and Letters, Vol. 27, No. 5, pp. 1950177, 2020.

[35] Aslantas, K., Ekici, E., Çiçek, A.: Optimization of process parameters for micro milling of Ti-6Al-4V alloy using Taguchi-based gray relational analysis, Measurement, Vol. 128, pp. 419-427, 2018.

[36] Mozammel, M.: Mathematical modeling and optimization of MQL assisted end milling characteristics based on RSM and Taguchi method, Measurement, Vol. 12, No. 1, pp. 249–260, 2018.

[37] FRCA FFICM, M.C, FRCA FFICM, M.A.: Statistical analysis: sample size and power estimations, BJA Education, Vol. 16, No. 5, pp. 159–161, 2016. https://doi.org/10.1093/bjaed/mkv0 34

[38] Jozić, S., Bajić, D., Celent, L.: Application of compressed cold air cooling: achieving multiple performance characteristics in end milling process, Journal of Cleaner Production, Vol. 100, pp. 325–332, 2015. https://doi.org/ 10.1016/j.jclepro.2015. 03.095

[39] Kalyon, A., Günay, M., Özyürek, D.: Application of grey relational analysis based on Taguchi method for optimizing machining parameters in hard turning of high chrome cast iron, Advances in Manufacturing, Vol. 6, pp. 419-429, 2018. https://doi.org/10.1007/s40436-018-0231-z

NOMENCLATURE

COF	Friction Coefficient
E	Young modulus (Gpa)
K	Thermal conductivity (J.m/m^2.s.°C)
Rc	Electrical resistance (mΩ)
X	Polarity
Y	Electrical current, I (A)
Z	Normal Load, P (N)
γ	Electrical resistivity [10^{-2} μΩm]
ρ	Density [g/cm3]

ОПТИМИЗАЦИЈА ПЕРФОРМАНСИ ТРЕЊА И ЕЛЕКТРИЧНОГ ОТПОРА У ЕЛЕКТРИЧНИМ КОНТАКТИМА ГРАФИТ-БАКАР КОРИШЋЕЊЕМ СИВЕ РЕЛАЦИОНЕ АНАЛИЗЕ ЗАСНОВАНЕ НА ТАГУЧИЈУ

Ђ. Бекхоуш, А. Боушуша, Х. Заиди

Ова студија има за циљ да истражи како оптерећење, интензитет и поларитет електричне струје утичу на понашање трења и електрични отпор између графитне игле оптерећене ротирајућим бакарним диском. Да би се то постигло, коришћен је трибометар са иглом на цилиндру. Релациона оцена сиве боје добијена из сиве релационе анализе је коришћена за процену карактеристике перформанси у Тагуцхи мешовитој Л18 (21 к 32) методи. Методом пројектовања Тагуцхи утврђени су оптимални контролни фактори који утичу на коефицијент трења и електрични отпор. Анализа варијансе (АНОВА) је коришћена за анализу утицаја контролних параметара на коефицијент трења и електрични отпор контакта. Параметри експеримента су укључивали примењено нормално оптерећење (3, 5,5 и 8,5 Н), електричну струју (10, 25 и 30 А) и поларитет (катода и анода). Резултати анализе су показали да је поларитет примарни фактор који утиче на коефицијент трења, док је електрична струја најефикаснији фактор електричног отпора контакта. Оптимални контролни параметри за постизање најнижих вредности коефицијента трења били су Кс1И331, док су за најниже вредности електричног отпора биле Кс2И333. На основу резултата сиве релационе анализе, оптимални параметри за минимизирање и коефицијента трења и електричног отпора били су Кс1И331.